Polymer(Korea), Vol. 41, No. 3, pp. 480-489 (2017)
https://doi.org/10.7317/pk.2017.41.3.480

ISSN 0379-153X(Print)
ISSN 2234-8077(Online)

키토산 기반 미세다공성 고분자의 Pd^{2+}에 대한 선택적 흡착성 및 재사용성

Jie Yu†, Jidong Zheng, Quanfang Lu*,†, Xing Wang, Xiaomin Zhang, Qizhao Wang, and Wu Yang

Key Lab of Bioelectrochemistry and Environmental Analysis of Gansu Province,
College of Chemistry and Chemical Engineering, Northwest Normal University
*Editorial Department of the University Journal, Northwest Normal University

(2016년 10월 31일 접수, 2017년 1월 5일 수정, 2017년 1월 7일 채택)

Selective Adsorption and Reusability for Pb^{2+} of Chitosan-based Microporous Polymer

Jie Yu†, Jidong Zheng, Quanfang Lu*,†, Xing Wang, Xiaomin Zhang, Qizhao Wang, and Wu Yang

Key Lab of Bioelectrochemistry and Environmental Analysis of Gansu Province, College of Chemistry and Chemical Engineering, Northwest Normal University, Lanzhou 730070, People's Republic of China

**Editorial Department of the University Journal, Northwest Normal University, Lanzhou 730070, People's Republic of China*

(Received October 31, 2016; Revised January 5, 2017; Accepted January 7, 2017)

Abstract: A green and simple glow-discharge electrolysis plasma (GDEP) technique was used to synthesize the chitosan/attapulgite/poly(acrylic acid-*co*-2-acrylamido-2-methyl-1-propanesulfonic acid) (CS/ATP/P(AA-*co*-AMPS)) microporous polymer. The results showed that the optimum pH for the adsorption of Pb^{2+}, Cd^{2+}, Co^{2+}, and Cu^{2+} is 4.8, and time of adsorption equilibrium is 60 min. Adsorption kinetics fits well to the pseudo-second-order model. The maximum adsorption capacities for Pb^{2+}, Cd^{2+}, Cu^{2+} and Co^{2+} are 500.0, 301.7, 180.0 and 151.7 mg g^{-1}, respectively. The microporous polymer has higher adsorption selectivity toward Pb^{2+} with the coexistence of Cd^{2+}, Co^{2+}, and Cu^{2+}. The CS/ATP/P(AA-*co*-AMPS) possesses promising regeneration and reusability using 2.0 g L^{-1} ethylenediamine tetraacetic acid tetrasodium salt (EDTA-4Na) solution as eluent. CS/ATP/P(AA-*co*-AMPS) can be used as a very promising absorbent for the separation, purification and selective recovery of Pb^{2+} in aqueous solution containing Cd^{2+}, Co^{2+}, and Cu^{2+} ions.

Keywords: chitosan, attapulgite, microporous polymer, adsorption selectivity, reusability.

Introduction

Heavy-metal ions are usually detected in some industrial wastewater, such as battery manufacturing, mining, metal plating, tannery, metallurgical industries, etc.[1] Pb, Cd, Cu and Co are the most common heavy metal pollutants which pose a threat to human health. Among those heavy metals, Pb, because of its considerable toxicological and environmental significances, is becoming a research focus in separation science and environmental contamination and remediation.[2] Therefore, effective removal of Pb^{2+} from waste water is great importance and necessity to environmental sustainability. Some methods, such as chemical precipitation,[3,4] chemical reduction,[5] reverse osmosis,[6] float membrane filtration[7] and adsorption[8-10] are widely used in removing and recovering Pb^{2+} from waste water. But the low selective separation is still a very large shortcoming using these methods. Hence, it is pressed for developing a good selective separation method and material for Pb^{2+}.

Chitosan (CS) is an abounding polymer in nature.[11] It is a deacetylated derivative of chitin and has excellent biocompatibility, biodegradability, adsorption activity and antimicrobial ability. As a result, CS has been generally used in the environmental, biomedical,[12] and agricultural fields.[13] CS is convenient to carry out modification because there are reactive -OH and $-NH_2$ in the structure of CS. Attapulgite (ATP) is a kind of layered hydrated magnesium aluminum silicate mineral and has excellent selective and regenerative ability in the waste water.[14]

Although CS and ATP have some advantages, their adsorp-

†To whom correspondence should be addressed.
E-mail: yujie741008@163.com; luqf@nwnu.edu.cn

tion capacity is very lower. For improving the adsorption properties, many functional groups, such as sulfate ($-SO_3^-$), carboxylate ($-COO^-$), sulfydryl (-SH), amino ($-NH_2$), were grafted onto these natural materials. In addition, in order to graft these active groups, various synthetic techniques are developed, such as thermal reaction,[15] microwave irradiation,[16] chemical initiators,[17-19] gamma radiation.[20,21] Roughly, radiation technique will produce secondary pollution having a great influence on the surrounding environment, meanwhile the setup is expensive.[21]

In recent year, a novel glow-discharge-electrolysis plasma (GDEP) technique has drawn much attention for preparation of polymers.[22,23] GDEP is a kind of non-equilibrium plasma, which can generate a large number of energetic species such as H·, HO·, O·, HO_2· and H_2O_2 in aqueous solutions. These active species would be initiated many polymerization reactions by free radical addition-crosslinking.[22-24]

Herein, the CS-based microporous polymer (chitosan/attapulgite/poly(acrylic acid-*co*-2-acrylamido-2-methyl-1-propanesulfonic acid) (CS/ATP/P(AA-*co*-AMPS)) was successfully synthesized by a simple one-step using GDEP technique in aqueous solution, in which *N*,*N*′-methylene-bis-acrylamide was used as a cross-linking agent. The structure, thermal stability, morphology and surface area of the microporous polymer were characterized by FTIR, TG-DTG, SEM and BET nitrogen adsorption-desorption. Then, the CS/ATP/P(AA-*co*-AMPS) was employed to remove the Pb^{2+}, Cd^{2+}, Cu^{2+} and Co^{2+} from aqueous solutions. The effect of pH on adsorption was optimized by batch experiments. The single-component adsorption kinetics and selective adsorption kinetics were investigated in detail. In addition, the desorption and reusability behaviors of the microporous polymer were discussed in various concentration ethylenediamine tetraacetic acid tetrasodium salt (EDTA-4Na) solution as eluent to explore the possibility for practical applications.

Experimental

Materials. Chitosan (CS, 85% degree of deacetylation) was supplied by Zhejiang Golden Shell Biological Chemistry Co., Ltd., China. Attapulgite (ATP, diameter of particles: 20-100 nm) is supplied by Jiuchuan Nano-material Technology Co., Ltd., Jiangsu, China. Acrylic acid (AA, analytical grade, Tianjin Guangfu Fine Chemical Research Institute, China) was distilled under reduced pressure before use. 2-Acrylamido-2-methyl-1-propanesulfonic acid (AMPS, analytical reagent grade, Shangdong Shouguang Runde Chemical Co., Ltd, China) was used without further purification. *N*,*N*′-methylene-bis-acrylamide (MBA, chemical pure, Shanghai Chemical Reagent Corporation, China) was used as received. Other chemicals, such as, $Pb(NO_3)_2$, $Co(NO_3)_2 \cdot 6H_2O$, $Cd(NO_3)_2 \cdot 4H_2O$, $Cu(NO_3)_2 \cdot 3H_2O$, NaOH, HNO_3 and ethylenediamine tetraacetic acid tetrasodium salt (EDTA-4Na) were all analytical grade reagents and supplied from Shanghai Chemical Reagent Corporation, China.

Preparation of CS/ATP/P(AA-*co*-AMPS) Microporous Polymer. CS/ATP/P(AA-*co*-AMPS) microporous polymer was synthesized according to our previous method.[23] 0.9 g CS and 0.4 g ATP were dispersed in 40 mL deionized water at 75 °C. Then, 2 g AMPS, 0.06 g MBA and 8 mL AA were added into the above mixture solution in order. The mixture was stirred for 20 min at 70 °C until the cross-linkers and monomers were dissolved completely. After that, two electrodes were inserted into the mixture solution to start the glow-discharge at 500 V for 2 min. Then, the reaction mixture was additionally stirred for 4 h, which was called the post polymerization of free radical initiation and chain addition reaction, followed by cooling the product to 25 °C. The milky product was obtained and cut into small piece. Then, the product was neutralized the -COOH and $-SO_3H$ groups with 1 mol L^{-1} NaOH solution to a degree of neutralization of about 80%. Finally, the product was washed 3 times with distilled water, dried in vacuum oven, milled through a 100-mesh sieve.

Characterizations of CS/ATP/P(AA-*co*-AMPS) Microporous Polymer. SEM and EDS measurements were carried out by an ULTRA plus FESEM field emission scanning electron microscope (Zeiss, Germany). Before SEM observation, the sample was coated with gold. The thermal stability of CS and CS/ATP/P(AA-*co*-AMPS) microporous polymer was determined by a PE TG/DTG 6300 instrument thermogravimetric analysis (PE, USA). The structure of the CS/ATP/P(AA-*co*-AMPS) microporous polymer was recorded on a Digilab FTS3000 FTIR spectrophotometer (Digilab, USA). The Brunauer-Emmett-Teller (BET) surface area (SBET) of the powder was analyzed by nitrogen adsorption in a Micromeritics ASAP 2020 nitrogen adsorption apparatus (USA). Metal ions concentration was analyzed three independent times using Varian 715-ES inductively coupled plasma-optical emission spectrometry (ICP-OES) (Varian Inc., USA). The pH values were performed with a PHS-3C Model pH meter (Inesa, China).

Effect of pH on Adsorption. The solution pHs for the

adsorption of Pb^{2+}, Cd^{2+}, Cu^{2+} and Co^{2+} were adjusted from 1.0 to 5.9 using 0.1 mg L^{-1} HNO_3 solution. 0.03 g of the CS/ATP/P(AA-*co*-AMPS) was added into a 100 mL single-component metal ion solution (300 mg L^{-1}), and was shaken with 140 r min^{-1} for 4 h. The adsorption capacity (Q_t) was calculated according to eq. (1):

$$Q_t = \frac{(C_0 - C_t)V}{m} \quad (1)$$

Where Q_t (mg g^{-1}) is the amount of heavy-metal ions taken up at any time, C_0 (mg L^{-1}) and C_t (mg L^{-1}) are the concentrations of the metal ions at initial and given time t (min). V (L) is the volume of the adsorption solution. m (g) is the mass of microporous polymers.

Single-component Adsorption Kinetics. 0.06 g of CS/ATP/P(AA-*co*-AMPS) was added into the 200 mL solution containing single-component heavy metal ions (300 mg L^{-1}, pH = 4.8) and was shaken with 140 r min^{-1} at 25 °C. Then, the supernatant solutions were taken at a specified time intervals and the concentration of heavy-metal ions was analyzed by ICP-OES. The adsorption capacity of heavy-metal ions was calculated by using the eq. (1).

Selective Adsorption. The selective adsorption of mixture solution (Pb^{2+}, Cd^{2+}, Co^{2+} and Cu^{2+} ions) containing equal molar concentration (i.e., 1.45 mmol L^{-1}) were performed at pH = 4.8 with 25 °C. A series of 0.06 g microporous polymer were added into 200 mL of mixture solution and shaken with 140 r min^{-1}. The supernatant solutions were taken within a certain period of time to determine the metal ions using ICP-OES.

Desorption and Reusability. A series of 0.03 g of microporous polymers were added into the Pb^{2+}, Cd^{2+}, Co^{2+} and Cu^{2+} ions solutions (300 mg L^{-1}, 100 mL, pH = 4.8) and shaken with 140 r min^{-1} for 4 h at 25 °C, respectively. Then, the solutions were measured using ICP-OES and the adsorption capacities were calculated according to the eq. (1). After that, CS/ATP/P(AA-*co*-AMPS) absorbed heavy-metal ions was moved into different concentration of EDTA-4Na desorption solution and stirred at 140 r min^{-1} for 4 h under 25 °C. Each ion concentration was analyzed using ICP-OES. The desorption capacity was measured from final heavy-metal ions concentration in the desorption solution. To test the reusability of the microporous polymer, repeated adsorption-desorption experiment was carried out 4 times.

The desorption ratio (η) was calculated according the following eq. (2):

$$\eta = \frac{Q_d}{Q_a} \times 100\% \quad (2)$$

Where η (%) is the desorption ratio, Q_d (mg g^{-1}) is the desorption capacity of heavy-metal ion desorbed into the elution medium, and Q_a (mg g^{-1}) is the adsorption capacity of heavy-metal ions adsorbed on the CS/ATP/P(AA-*co*-AMPS).

Results and Discussion

Polymerization Mechanism. The GDEP can produce several reactive species in aqueous solution such as HO·, H· and O· radicals, among which HO· is one of the strongest oxidants ($E^0_{HO\cdot/H_2O}$= 2.85 V).[25] Therefore, HO· radicals play the most important role in inducing chemical reactions in GDEP. Generally speaking, apart from hydrogen abstraction on labile H of hydrocarbon chains ($HO\cdot + RH \rightarrow H_2O + R\cdot$), HO· can also participate in electrophilic addition to unsaturated bond:[26]

$$HO\cdot + R_2C = CR_2 \rightarrow R_2(OH)C\text{-}CR_2\cdot$$

Thus, in the induced copolymerization of CS, ATP, AA and AMPS by GDEP, reactions of the hydrogen abstraction from CS and ATP, and the electrophilic addition of AA and AMPS are simultaneously existed. The proposed mechanism of synthesized the CS/ATP/P(AA-*co*-AMPS) by GDEP is showed in Scheme 1. At first, H_2O molecules can be dissociated into HO·, H· and O· radicals by the energetic electrons from GDEP, which is called the radicals forming process (reaction 1). Then, HO· can react with labile H from CS and ATP by abstraction of hydrogen to form the new organic radical (a, b and c). Meanwhile, HO· radicals can also add to unsaturated C=C bonds of AA and AMPS forming the new organic radicals (d). The above reactions are called the chain initiation process (reaction 2). After that, these radicals (a, b, c and d) optionally react with AA and AMPS monomers to produce macromolecule free radicals (e, f, g and h), and lead to the chain propagation (reaction 3). Finally, reactions of macromolecule radicals are terminated by crosslinking copolymerization of crosslinking agent MBA, radical-radical combinations, and disproportionations to form a three-dimensional network copolymer which is called the termination reaction (reaction 4).[22-24] And then, copolymers are neutralized the -COOH and -SO_3H of the grafted poly(acrylic acid) (PAA) and poly(2-acrylamido-2-methyl-1-propanesulfonic acid) (PAMPS), and the resulting product is obtained (reaction 4). So we can say

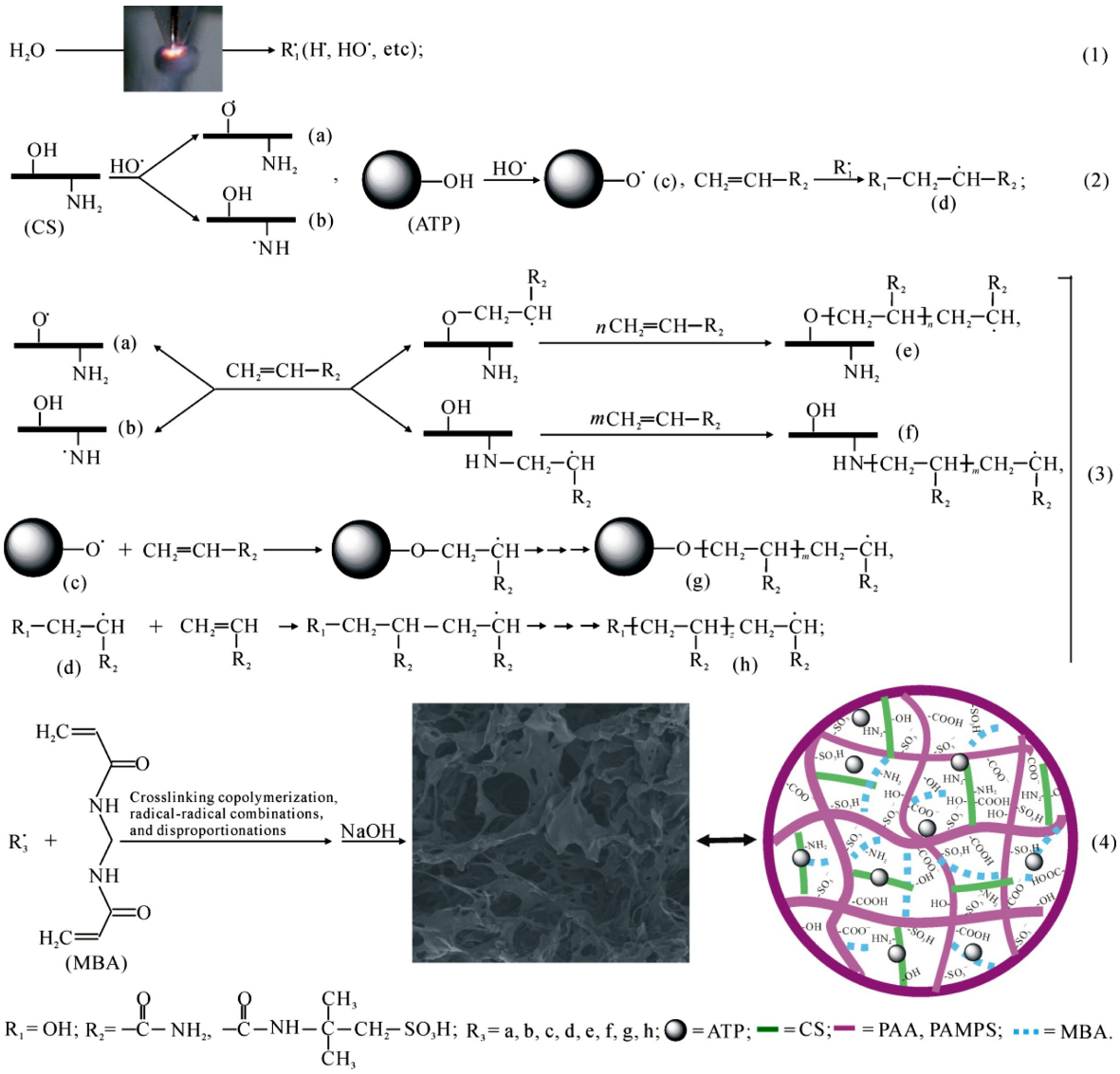

Scheme 1. Copolymerization mechanism of CS/ATP/P(AA-*co*-AMPS) induced by GDEP: (1) radical formation; (2) chain initiation; (3) chain propagation; (4) chain termination and neutralization of PAA and PAMPS.

that copolymerization mechanism initiated by GDEP is a free radical addition-crosslinking reaction.

Characterizations of CS/ATP/P(AA-*co*-AMPS) Microporous Polymer. The FTIR spectra of CS (a), ATP (b), AA (c), AMPS (d) and CS/ATP/P(AA-*co*-AMPS) (e) are showed in Figure 1. The main characteristic peaks of CS (a) are 3437 cm^{-1} (N-H and O-H stretch), 2872 cm^{-1} (C-H stretch), 1599 cm^{-1} (NH_2 bend), 1326 cm^{-1} (C-N stretch), and 1172 cm^{-1} (bridge O stretch).[24] The main characteristic peak of ATP (b) is 1027 cm^{-1} (Si-O-Si stretch). The main characteristic peaks of AA (c) are 1705 cm^{-1} (C=O stretch) and 1631 cm^{-1} (C=C stretch). The main characteristic peaks of AMPS (d) are 3245 cm^{-1} (N-H stretch), 1663 cm^{-1} (C=O of amide stretch), 1607 cm^{-1} (C=C stretch), 1366 cm^{-1} (C-N stretch) and 1244 cm^{-1} (SO_2 asymmetric stretch).[22,24] In the FTIR spectrum of CS/ATP/P(AA-*co*-AMPS) (e), the peaks such as 1599 cm^{-1} (NH_2 bend) of CS, 1632 cm^{-1} (C=C stretch) of AA and 1607 cm^{-1} (C=C stretch) of AMPS disappeared. Meanwhile, new absorption peaks at 1567 cm^{-1} (C=O of $-COO^-$ asymmetric stretch),[23] 1220 cm^{-1} (SO_2 asymmetric stretch)[24] and 1044 cm^{-1} (Si-O-Si stretch)[27] appeared. The above information indicates that $-NH_2$ of CS is taken part in the grafting reaction, AMPS and AA have been grafted onto the CS backbone by using GDEP, and ATP has been adulterated into the microporous polymer.

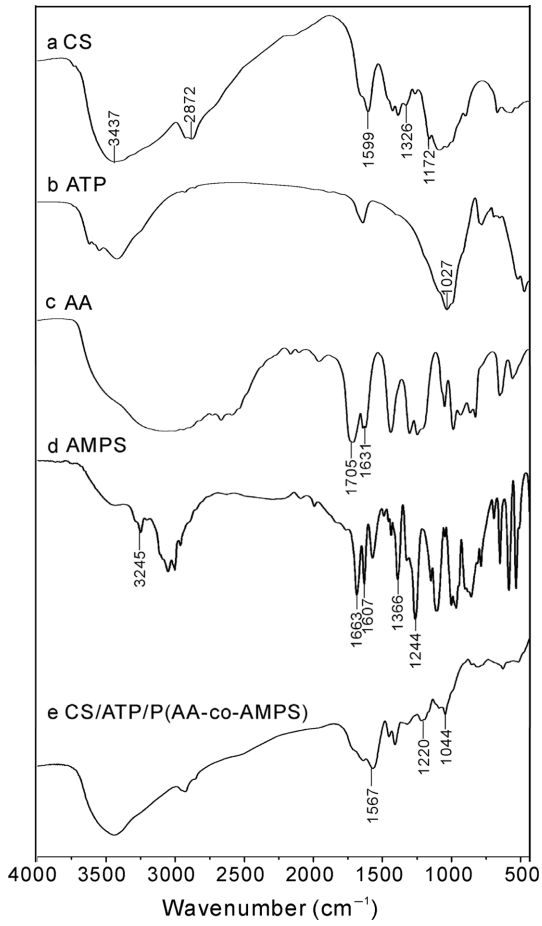

Figure 1. FTIR spectra of (a) CS; (b) ATP; (c) AA; (d) AMPS; (e) CS/ATP/P(AA-*co*-AMPS) microporous polymer.

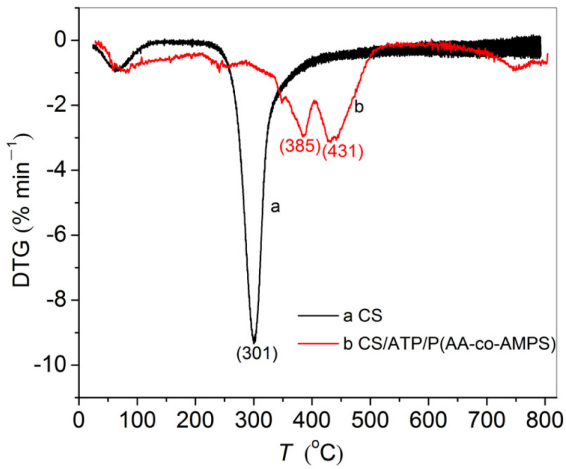

Figure 2. DTG curves of CS (a); CS/ATP/P(AA-*co*-AMPS) microporous polymer (b).

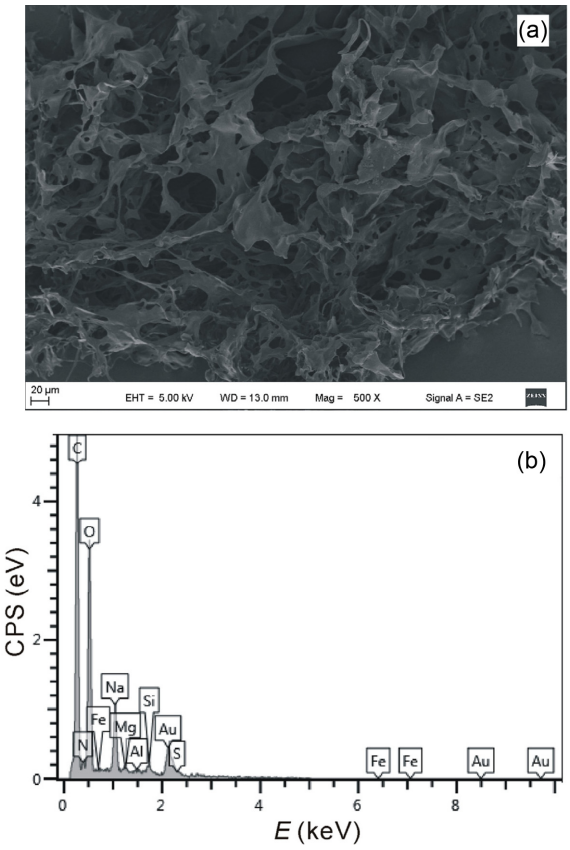

Figure 3. SEM (a); EDS (b) of CS/ATP/P(AA-*co*-AMPS) microporous polymer.

Thermal stability of CS and CS/ATP/P(AA-*co*-AMPS) microporous polymer was assessed by DTG analysis. As showed in Figure 2, the maximum decomposition temperature (T_{max}) of CS is 301 ºC. This could be attributed to the dehydration of the saccharide rings and the decomposition of the deacetylated and acetylated units of chitosan.[24] However, the T_{max} of CS/ATP/P(AA-*co*-AMPS) microporous polymer increased to 385 and 431 ºC. This is ascribed to the decomposition of grafted CS, the breakage of crosslinking network structure and the decomposition of grafted P(AA-*co*-AMPS) chain in polymeric backbone, respectively.[28] In addition, the decomposition rate is lesser than CS. This indicated that CS/ATP/P(AA-*co*-AMPS) microporous polymer forms a more stable structure.

SEM micrograph of microporous polymer is showed in Figure 3(a). The CS/ATP/P(AA-*co*-AMPS) shows a network structure with many irregular folds and holes. This unique surface is good for diffusing metal ions into the polymeric networks to obtain a rapid adsorption rate.[22] As showed in Figure 3(b) from EDS, the signals of Al, Fe, Mg and Si elements can be detected from the structure. It further suggests that ATP has been adulterated into the microporous polymer, which is in accord with the FTIR results.

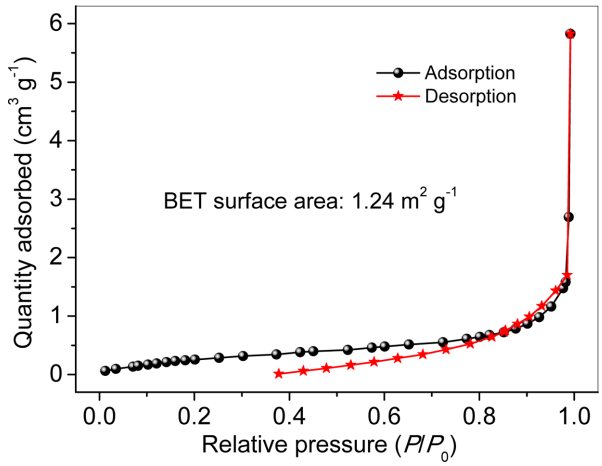

Figure 4. Nitrogen adsorption-desorption isotherm of the CS/ATP/P(AA-*co*-AMPS) polymer.

BET nitrogen adsorption-desorption was performed to determine the specific surface area of the CS/ATP/P(AA-*co*-AMPS) polymer. As showed in Figure 4, the BET surface area of the CS/ATP/P(AA-*co*-AMPS) polymer is 1.24 m^2 g^{-1}.

Effect of pH on Adsorption. The pH is one of the most important parameters which affect the surface charge of the active adsorption sites and the degree of ionization.[29] The adsorption of heavy-metal ions on adsorbent was investigated over the pH = 1.0-5.9 because heavy-metal ions could be precipitated by OH^- to form metal hydroxide above pH 6.0.[24] Figure 5 shows the adsorption capacity of CS/ATP/P(AA-*co*-AMPS) for Pb^{2+}, Cd^{2+}, Cu^{2+} and Co^{2+} at pH ranged from 1.0 to 5.9. At lower pH value (pH<2), protons compete with heavy metal ions for the active adsorption sites, and the sulfonate and carboxylate groups are protonated to block the chelation interaction between these groups and heavy metal ions.[29,30] This fact can lead to the low uptake of Pb^{2+} ions and even no appreciable uptake of Cd^{2+}, Cu^{2+} and Co^{2+}. With increasing the pH from 2 to 4.8, the competition from H^+ is gradually weakened,[31] and the protonation degree of adsorption groups is decreased, the interactions of ion exchange and chelation can be significantly increased, and the adsorbed capacities of all metal ions are increased. Further increase of pH from 4.8 to 5.9, the adsorbed capacity of Pb^{2+} decreased and the adsorbed capacities of Cd^{2+}, Cu^{2+} and Co^{2+} mainly remained about the same. This is because higher pH can lead to combination or precipitation between Pb^{2+} ions and OH^-.[30] The adsorbed capacity of Pb^{2+} is obviously higher than other three ions in the pH studied ranges, implying possible selectivity for Pb^{2+} ions is produced. In order to study the comparative adsorption of metal ions on CS/ATP/P(AA-*co*-AMPS), pH = 4.8 was chosen as the optimum pH.

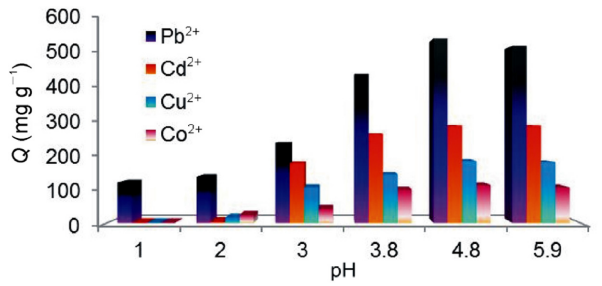

Figure 5. Effect of pH on adsorption for heavy metal ions by CS/ATP/P(AA-*co*-AMPS).

Single-component Adsorption Kinetics. The adsorption kinetics on the single-component of Pb^{2+}, Cd^{2+}, Cu^{2+} and Co^{2+} ions at 300 mg L^{-1} initial concentration is studied. As showed in Figure 6, the adsorption capacity increases sharply in initial 5 min, then becomes slowly from 10 to 30 min, and finally reaches equilibrium within 60 min. The equilibrium adsorption capacities of Pb^{2+}, Cd^{2+}, Cu^{2+} and Co^{2+} ions are 500.0, 301.7, 180.0 and 151.7 mg g^{-1}, respectively. The results suggested that CS/ATP/P(AA-*co*-AMPS) has quite fast adsorption rate and high adsorption capacities. This is because all the adsorbent sites are vacant and the metal ions concentrations are high in the beginning fast adsorption.[32] Then, the available sites in the adsorbent reduce and thus rates of adsorption decrease.[33] Finally, all adsorbent sites are occupied and the adsorption process reaches equilibrium.

Quantitative kinetic analysis is important for adsorption process design and can get the rate of adsorption, the rate-con-

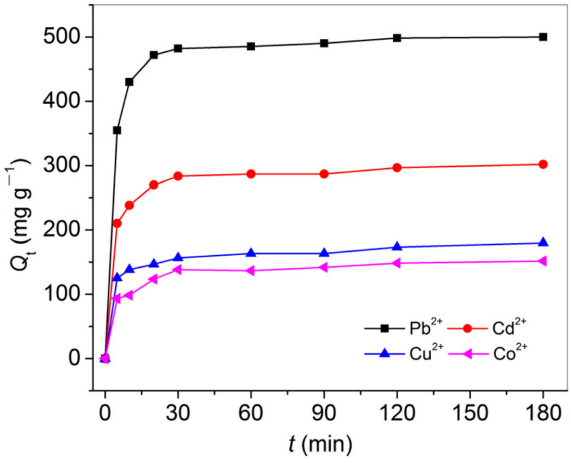

Figure 6. Effect of contact time on the single-component adsorption for heavy metal ions by CS/ATP/P(AA-*co*-AMPS) at pH=4.8.

trolling step of adsorption, and the adsorption mechanism.[31] The pseudo-second-order equation is often used to describe CS-pollutants systems.[24,33] It is in agreement with chemisorption, and the adsorption rate is controlled by chemical adsorption through sharing or exchange of electrons between the metal ions and polymer.[34] It is expressed as:

$$\frac{t}{Q_t} = \frac{1}{kQ_e^2} + \frac{t}{Q_e} \quad (3)$$

Where k (g mg^{-1} min^{-1}) is the rate constant of the pseudo-second-order model. The intercept ($1/kQ_e^2$) and slope ($1/Q_e$) of t/Q_t *versus* t (Figure 7) can be used to obtain the parameters of k and Q_e (Table 1).

Figure 7 indicates that the experimental data give the excellent agreement with the pseudo-second-order model. The linear correlation coefficients (R^2) of all metal ions are above 0.99 (Table 1). Moreover, the calculated Q_e values (Pb^{2+} 505.1 mg g^{-1}, Cd^{2+} 304.0 mg g^{-1}, Cu^{2+} 181.2 mg g^{-1} and Co^{2+} 154.6 mg g^{-1}) are exactly consistent with the experimental $Q_{e,exp}$ values (Pb^{2+} 500.0 mg g^{-1}, Cd^{2+} 301.7 mg g^{-1}, Cu^{2+} 180.0 mg g^{-1} and Co^{2+} 151.7 mg g^{-1}). These findings indicate that the adsorption process of four ions on CS/ATP/P(AA-*co*-AMPS) are conformed to the pseudo-second-order kinetic model and the adsorption process is mainly controlled by a chemical adsorption.

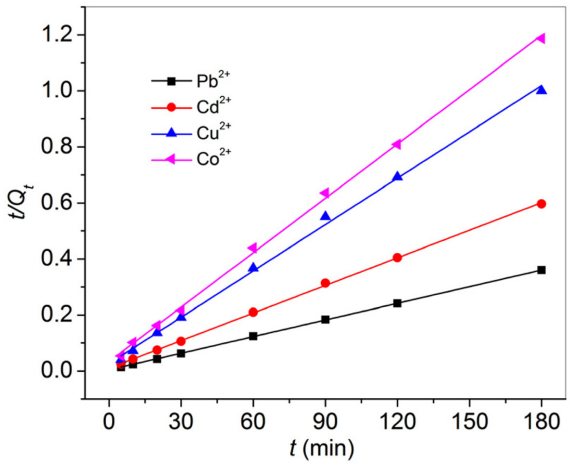

Figure 7. Pseudo-second-order kinetics model of Pb^{2+}, Cd^{2+}, Cu^{2+} and Co^{2+} on CS/ATP/P(AA-*co*-AMPS).

Table 1. Pseudo-second-order Kinetic Parameters for Adsorption of Pb^{2+}, Cd^{2+}, Cu^{2+} and Co^{2+} Ions on CS/ATP/P(AA-*co*-AMPS) in the Single-component Solution

Metal ions	$Q_{e,exp}$ (mg g^{-1})	Pseudo-second-order model		
		$k\times10^{-3}$ (g mg^{-1} min^{-1})	Q_e (mg g^{-1})	R^2
Pb^{2+}	500.0	1.062	505.1	0.9999
Cd^{2+}	301.7	1.119	304.0	0.9996
Cu^{2+}	180.0	1.164	181.2	0.9978
Co^{2+}	151.7	1.230	154.6	0.9989

Selective Adsorption. The inset (a-e) of Figure 8 is corresponded to the photographs of dry CS/ATP/P(AA-*co*-AMPS) (a), adsorption Cu^{2+} (b), Co^{2+} (c), Pb^{2+} (d) and adsorption Cu^{2+} ,Co^{2+}, Cd^{2+} and Pb^{2+} in the mixture solution by CS/ATP/P(AA-*co*-AMPS) (e). As showed in inset of Figure 8, the CS/ATP/P(AA-*co*-AMPS) is milky product. After adsorption of Cu^{2+} and Co^{2+}, the color of the solutions of Cu^{2+} (b), Co^{2+} (c) are obviously colorless and the adsorbents are accordingly presented the color of metal ions. However, there is no remarkable color change in Figure 8(d) because Pb^{2+} is colourless. It can be seen with the naked eye that the color of polymer in mixed solution became less blue, which suggested that only a small part of Cu^{2+} in solution was adsorbed by CS/ATP/P(AA-*co*-AMPS).

Figure 8 shows the kinetic curves of the multi-components mixture solution of Pb^{2+}, Cd^{2+}, Co^{2+} and Cu^{2+} ions with 1.45 mmol L^{-1} at pH = 4.8 and 25 °C. As showed in Figure 8, the adsorption capacity of Cd^{2+}, Cu^{2+} and Co^{2+} ions increases sharply at initial 10 min, then decreases gradually from 30 to 90 min, and finally levels off after 180 min. Obviously, the initially adsorbed Cd^{2+}, Cu^{2+} and Co^{2+} ions on CS/ATP/P(AA-*co*-AMPS) are subsequently released into the solution in the

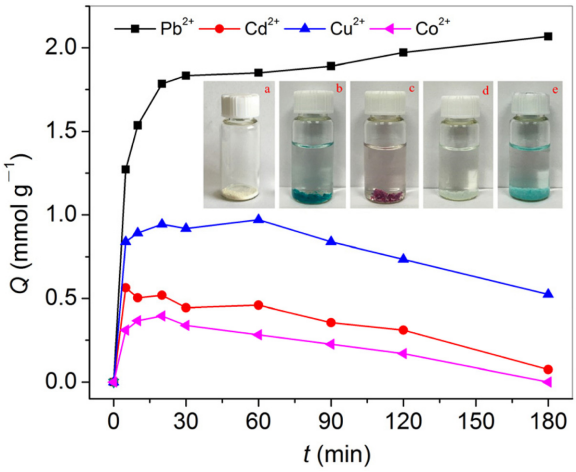

Figure 8. Selective adsorption of Pb^{2+} with the coexistence of Cd^{2+}, Cu^{2+} and Co^{2+} on CS/ATP/P(AA-*co*-AMPS). Inset: Color of microporous polymers of dry (a); after adsorption of Cu^{2+} (b); Co^{2+}(c); Pb^{2+} (d) in single-component solution; (e) mixture solution.

multi-components adsorption process. However, the adsorption capacity of Pb^{2+} is increased until 180 min. The most possible explanation of this result is the equilibrium constants between chelating group and Pb^{2+} has higher than that of Cd^{2+}, Cu^{2+} and Co^{2+}. If one metal ions complex is more stable than another of the same type, a metal ions will displace another form a higher stable complex.[35] That is to say, when the Pb^{2+} ions diffuse to the chelating sites of CS/ATP/P(AA-*co*-AMPS), they can replace Cd^{2+}, Cu^{2+} and Co^{2+} of adsorbed. When the CS/ATP/P(AA-*co*-AMPS) was added into the mixture solution, all metal ions had the opportunities to occupy the chelating sites because a large number of unreacted chelating groups was existed in adsorbent. When the chelating sites were occupied by adsorbed heavy metal ions, no metal ions could diffuse toward the adsorption sites except Pb^{2+}.[22] It can be seen clearly that the adsorbed capacity of Pb^{2+} is higher than that of the other ions at all time, and the adsorption capacity follows the order: $Pb^{2+}>Cu^{2+}>Cd^{2+}>Co^{2+}$. It suggests that CS/ATP/P(AA-*co*-AMPS) microporous polymer has outstanding adsorption selectivity for Pb^{2+} after a proper adsorption time.

The selectivity coefficient α and distribution coefficients K_d (mL g^{-1}) can be used to reflect the stability of a metal-ligand complex.[22] The higher the α and K_d value are, the more stable the metal-ligand complex is. The high α and K_d values of metal ions are also favorable because they indicate the high affinity of the adsorbent with the metal ions.[22,36] The K_d and α are given by:

$$K_d = \frac{C_0 - C_e}{C_0} \cdot \frac{V}{m} \quad (4)$$

$$\alpha = \frac{K_d(Pb^{2+})}{K_d(M^{2+})} \quad (5)$$

Where C_0 and C_e(mg L^{-1}) are the concentrations of metal ions before and after adsorption, respectively. V(L) is the volume of solution and m(g) is the mass of microporous polymer. K_d (Pb^{2+}) is the distribution coefficient of Pb^{2+} ions, and $K_d(M^{2+})$ is the distribution coefficient of Cd^{2+}, Cu^{2+} and Co^{2+} ions, respectively.

The equilibrium adsorption capacities (Q), K_d and α values of CS/ATP/P(AA-*co*-AMPS) in 1.45 mmol L^{-1} mixture solution are listed in Table 2. As can be seen from Table 2, the Q and K_d values of Pb^{2+} are highest. The values of α are 4.67 and 6.11. Therefore, the CS/ATP/P(AA-*co*-AMPS) has good adsorption selectivity for Pb^{2+} with the coexistence of Cu^{2+}, Cd^{2+}, and Co^{2+}.

Table 2. Equilibrium Adsorption Capacities (Q), the Distribution Coefficient K_d (mL g^{-1}) and Selectivity Coefficient α for Pb^{2+} *versus* Other Metal Ions on CS/ATP/P(AA-*co*-AMPS) at 180 min in the Multi-component Mixture Solution

Metal ions	Q (mmol g^{-1})	K_d (mL g^{-1})	α
Pb^{2+}	2.067	2191	-
Cd^{2+}	0.0741	469	4.67
Cu^{2+}	0.5245	358. 4	6.11
Co^{2+}	0	0	∞

Table 3. Desorption Ratios of Pb^{2+}, Cd^{2+}, Cd^{2+} and Co^{2+} Ions in Different Concentration of EDTA-4Na

Concentration of EDTA-4Na (g L^{-1})	Desorption ratio (%)			
	Pb^{2+}	Cd^{2+}	Cu^{2+}	Co^{2+}
0.2	28.8	46.5	61.2	58.3
0.6	45.6	64.4	69.6	86.9
1.0	71.9	72.4	90.0	91.6
2.0	90.2	88.1	93.6	93.7

Desorption and Reusability. In order to study the practical application of CS/ATP/P(AA-*co*-AMPS) in wastewater treatment, the reusability of adsorbent is very meaningful.[37] EDTA-4Na is a very strong chelating agent for some metal ions, it can replace the functional groups on the CS/ATP/P(AA-*co*-AMPS) microporous polymer and chelate heavy metal ions.[38] Therefore, EDTA-4Na was thought to be one of the most suitable eluent for heavy metal ions.[39,40] Furthermore, the optimum concentration is necessary to avoid excessive EDTA-4Na leading to a waste and uneconomical. Table 3 indicated that the desorption ratio of metal ions increased with the increasing EDTA-4Na concentration. Moveover, the desorption ratio of those metal ions using 2.0 g L^{-1} EDTA-4Na was more than 88%. Hence, the optimum concentration of EDTA-4Na was 2.0 g L^{-1} for economical reason.

Figure 9 shows the reusability of the CS/ATP/P(AA-*co*-AMPS) microporous polymer via four sequential cycles of adsorption-desorption experiment using 2.0 g L^{-1} EDTA-4Na as eluent. In repeated adsorption process, the adsorption capacities of all ions were slightly higher than that of the first cycle. The increased adsorption capacity of all ions is ascribed to the following reasons: the grafted microporous polymer has been neutralized of a degree of about 80% while most of $-SO_3H$ and -COOH has been converted into $-SO_3Na$ and -COONa. The Na^+ ions were exchanged with the metal ions in the course of adsorption. On the contrary, the adsorbed metal ions were exchange with Na^+ in desorption process. Meanwhile, -COOH

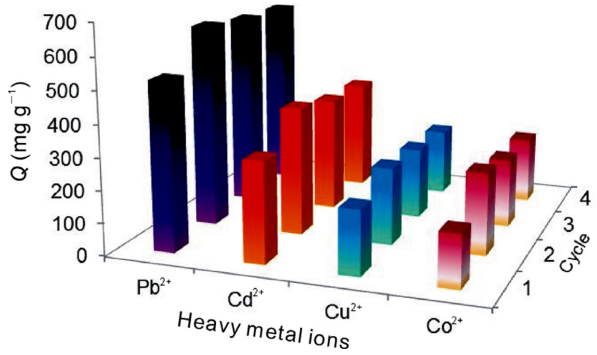

Figure 9. Adsorption capacities of Pb^{2+}, Cd^{2+}, Cd^{2+} and Co^{2+} at sequential four adsorption-desorption cycles using 2.0 g L^{-1} EDTA-4Na as eluent.

and -SO_3H are weak acid who have an ionization equilibrium in water solution.

$$\text{-COOH} \rightleftharpoons \text{-COO}^- + \text{H}^+$$
$$\text{-SO}_3\text{H} \rightleftharpoons \text{-SO}_3^- + \text{H}^+$$

EDTA-4Na makes the ionization equilibrium move forward and unneutralized -COOH and -SO_3H are activated, so the repeated adsorption capacities of all metal ions are slightly higher than first. It suggests that the CS/ATP/P(AA-*co*-AMPS) microporous polymer has a good reusability and is a promising candidate for practical application in wastewater treatment. EDTA-4Na is an excellent desorption solution for CS/ATP/P(AA-*co*-AMPS) absorbed heavy metal ions.

Conclusions

A novel sulfate (-SO_3^-) and carboxylate (-COO^-) functionalized microporous polymer chitosan/attapulgite/poly(acrylic acid-*co*-2-acrylamido-2-methyl-1-propanesulfonic acid) (CS/ATP/P(AA-*co*-AMPS)) was successfully synthesized using GDEP technique for efficient removal of Pb^{2+}, Cd^{2+}, Cu^{2+} and Co^{2+} ions. The copolymerization mechanism initiated by GDEP is a free radical addition-crosslinking reaction. SEM showed that the microporous polymer presents a three dimensional network microstructure and has many pores. TG/DTG analysis indicated that CS/ATP/P(AA-*co*-AMPS) microporous polymer forms a more stable structure compared with CS. FTIR spectra analysis revealed that -NH_2 of CS takes part in grafting reaction and, AMPS and AA have been grafted onto the CS backbone. The EDS suggested that ATP has been adulterated into the microporous polymer. BET nitrogen adsorption-desorption showed that the BET surface area of CS/ATP/P(AA-*co*-AMPS) is 1.24 m^2 g^{-1}. The optimum pH of adsorption for heavy metal ions is pH 4.8, and the adsorption equilibrium is 60 min. The adsorption process is agreed well with the pseudo-second-order equation. The capacities for Pb^{2+}, Cd^{2+}, Cu^{2+} and Co^{2+} ions are 500.0, 301.7, 180.0 and 151.7 mg g^{-1}, respectively. In addition, the microporous polymer has promising adsorption selectivity towards Pb^{2+} with the coexistence of Cd^{2+}, Co^{2+}, and Cu^{2+} ions. Moreover, the CS/ATP/P(AA-*co*-AMPS) displays excellent regeneration and reusability using 2.0 g L^{-1} EDTA-4Na as eluent. All results suggested that the CS/ATP/P(AA-*co*-AMPS) polymer has large adsorption capacities, promising reusability, and high selectivity for Pb^{2+}. It can be used as a very promising absorbent for the separation, purification, and selective recovery of Pb^{2+} with the coexistence of Cd^{2+}, Co^{2+}, and Cu^{2+} ions systems. In addition, this study also shows that GDEP may provide a new approach for the preparation and development of CS-based high-performance microporous polymer.

Acknowledgements: This work was supported in part by National Natural Science Foundation of China (Nos. 21367023 and 21567025), and Natural Science Foundation of Gansu Province (Nos. 1308RJZA144 and 1208RJZA161).

References

1. N. Li, R. B. Bai, and C. K. Liu, *Langmuir*, **21**, 11780 (2005).
2. S. Ghoohestani and H. Faghihian, *Desalin. Water. Treat.*, **57**, 4049 (2016).
3. Y. M. Liu, X. J. Ju, Y. Xin, W. C. Zheng, W. Wang, J. Wei, R. Xie, Z. Liu, and L. Y. Chu, *ACS Appl. Mater. Interfaces*, **6**, 9530 (2014).
4. F. Fu, L. Xie, B. Tang, Q. Wang, and S. Jiang, *Chem. Eng. J.*, **189-190**, 283 (2012).
5. Y. Ying, Y. Liu, X. Wang, Y. Mao, W. Cao, P. Hu, and X. Peng, *ACS Appl. Mater. Interfaces*, **7**, 1795 (2015).
6. H. Ozaki, K. Sharma, and W. Saktaywin, *Desalination*, **144**, 287 (2002).
7. C. Blöcher, J. Dorda, V. Mavrov, H. Chmiel, N. K. Lazaridis, and K. A. Matis, *Water. Res.*, **37**, 4018 (2003).
8. H. A. Essawy and H. S. Ibrahim, *React. Funct. Polym.*, **61**, 421 (2004).
9. R. Khalili, F. Shabanpoue, and H. Eisazadeh, *Adv. Polym. Technol.*, **33**, 21389 (2014).
10. V. S. Nguyen and T. Y. L. Ho, *J. Chem. Technol. Biotechnol.*, **88**, 1641 (2013).
11. B. Tanhaei, A. Ayati, F. F. Bamoharram, M. Lahtinen, and M. Sillanp, *J. Chem. Technol. Biotechnol.*, **91**, 1452 (2016).

12. J. K. Park, J. W. Nah, and C. Choi, *Polym. Korea*, **39**, 480 (2015).
13. N. M. Alves and J. F. Mano, *Int. J. Biol. Macromol*., **43**, 401 (2008).
14. J. R. Qu, J. J. Zhang, Y. F. Gao, and H. Yang, *Food Chem*., **135**, 1148 (2012).
15. H. Ge and S. Wang, *Carbohydr. Polym*., **113**, 296 (2014).
16. G. Huacai, P. Wan, and L. Dengke, *Carbohydr. Polym*., **66**, 372 (2006).
17. J. Zhang, Q. Wang, and A. Wang, *Carbohydr. Polym*., **68**, 367 (2007).
18. J. M. Joshi and V. K. Sinha, *Polymer*, **47**, 2198 (2006).
19. H. Hosseinzadeh and D. Alijani, *Polym. Korea*, **38**, 588 (2014).
20. N. M. El-Sawy, H. A. A. El-Rehim, A. M. Elbarbary, and E. S. A. Hegazy, *Carbohydr. Polym*., **79**, 555 (2010).
21. M. H. Casimiro, M. L. Botelho, J. P. Leal, and M. H. Gil, *Radiat. Phys. Chem*., **72**, 731 (2005).
22. J. Yu, J. D. Zheng, Q. F. Lu, S. X. Yang, X. M. Zhang, X. Wang, and W. Yang, *Colloid Polym. Sci*., **294**, 1585 (2016).
23. J. Yu, G. G. Yang, Y. P. Pan, Q. F. Lu, W. Yang, and J. Z. Gao, *Plasma Sci. Technol*., **16**, 767 (2014).
24. J. Yu, Y. Li, Q. F. Lu, J. D. Zheng, S. X. Yang, F. Jin, Q. Z. Wang, and W. Yang, *Iran Polym. J*., **25**, 423 (2016).
25. R. P. Joshi and S. M. Thagard, *Plasma Chem. Plasma Process*., **33**, 17 (2013).
26. J. L. Brisset, D. Moussa, A. Doubla, E. Hnatiuc, B. Hnatiuc, G. K. Youbi, J. M. Herry, M. Naïtali, and M. N. Bellon-Fontaine, *Ind. Eng. Chem. Res*., **47**, 5761 (2008).
27. J. Liu, Q. Wang, and A. Wang, *Carbohydr. Polym*., **70**, 166 (2007).
28. L. Qian and H. Zhang, *Green Chem*., **12**, 1207 (2010).
29. A. Heidari, H. Younesi, Z. Mehraban, and H. Heikkinen, *Int. J. Bio. Macromol*., **61**, 251 (2013).
30. G. Zeng, Y. Pang, Z. Zeng, L. Tang, Y. Zhang, Y. Liu, J. Zhang, X. Lei, Z. Li, Y. Xiong, and G. Xie, *Langmuir*, **28**, 468 (2012).
31. J. He, Y. Lu, and G. Luo, *Chem. Eng. J*., **244**, 202 (2014).
32. I. A. Sengil and M. Ozacar, *J. Hazard. Mater*., **166**, 1488 (2009).
33. M. Kumar, B. P. Tripathi, and V. K. Shahi, *J. Hazard. Mater*., **172**, 1041 (2009).
34. Y. Liu, Z. Liu, J. Gao, J. Dai, J. Han, Y. Wang, J. Xie, and Y. Yan, *J. Hazard. Mater*., **186**, 197 (2011).
35. C. Y. Chen and S. Y. Chen, *J. Appl. Polym. Sci*., **94**, 2123 (2004).
36. X. Xiao, F. Hayashi, H. Shiiba, S. Selcuk, K. Ishihara, K. Namiki, L. Shao, H. Nishikiori, A. Selloni, and K. Teshim, *J. Phys. Chem. C*, **120**, 11984 (2016).
37. R. Laus, T. G. Costa, B. Szpoganicz, and V. T. Fávere, *J. Hazard. Mater*., **183**, 233 (2010).
38. C. Jeon and K. H. Park, *Water Res*., **39**, 3938 (2005).
39. W. S. W. Ngah, L. C. Teong, R. H. Toh, and M. Hanafiah, *Chem. Eng. J*., **209**, 46 (2012).
40. Y. Y. Xu, Q. F. Dang, C. S. Liu, J. Q. Yan, B. Fan, J. P. Cai, and J. J. Li, *Colloid Surf. A*, **482**, 353 (2015).